Journal of Advances in Applied Mathematics, Vol. 6, No. 3, July 2021
https://dx.doi.org/10.22606/jaam.2021.63001

Controlling Chaotic Vibrations of a Quarter-Car Model Excited by Road Surface Profile using Parametric Excitation.

Lawrence Atepor[1], Richard Nii Ayitey Akoto[2]

[1] Department of Mechanical Engineering, Cape Coast Technical University, Cape Coast, Ghana.
[2] School of Graduate Studies, University of Professional Studies, Box LG 149, Accra, Ghana.
Email: cprector@gmail.com

Abstract. Chaotic Vibrations are considered for a quarter-car model excited by the road surface profile. The equation of motion is obtained in the form of a classical Duffing equation and it is modeled with deliberate introduction of parametric excitation force term to enable us manipulate the behavior of the system. The equation of motion is solved using the Method of Multiple Scales. The steady-state solutions with and without the parametric excitation force term is investigated using NDSolve *Mathematica*^{TM} Code and the nonlinear dynamical system's analysis is by a study of the Bifurcations that are observed from the analysis of the trajectories, and the calculation of the Lyapunov. In making the system more strongly nonlinear the excitation amplitude value is artificially increased to various multiples of the actual value. Results show that the system's response can be extremely sensitive to changes in the amplitude and the that chaos is evident as the system is made more nonlinear and that with the introduction of parametric excitation force term the system's motion becomes periodic resulting in the elimination of chaos and the reduction in amplitude of vibration.

Keywords: chaotic vibration, parametric excitation, excitation frequency, quarter-car, magnetorheological dampers.

1 Introduction

Suspension is the system of tires, tire air, springs, shock absorbers, and linkages that connects a vehicle to its wheels and allows them to move relative to one another. Suspension systems are meant to serve a dual purpose: they are to contribute to the vehicle's road holding/handling and braking for good active safety and driving pleasure, as well as they keep vehicle occupants comfortable and a ride quality that is reasonably well isolated from road noise, bumps, vibrations, and so on.

Unwanted vibrations due to kinematic excitations from rough surface road profiles are still of research interest to scientists and inventors, whose aim is to reduce the effect of vehicle's vibrations on drivers and passengers, [1] and [2]. Many researchers have studied new applications of active and semi-active control procedures and special devices to reduce vehicle vibrations, Guo et.al.[3] and Lauwerys et.al.[4] Szabelski & Samodulski [5] and Mitschke [6] re-examined old mechanical quarter-car models in the context of active damper applications. Authors like Choi & Lee [7] and Lai & Liao [8] have deduced that dampers based on magnetorheological fluid with typical hysteretic characteristics have significant promise for effective vibration damping in many applications. Other vehicle vibration damping methods such as 'Sky hook' control or H ∞ control have been proposed and tested in several car applications by [9] and [10]. Dixit & Borse [11] and Allamraju [12] advanced the argument that suspensions are basically required to provide a high level of ride comfort while maintaining a reasonable ability to ensuring safety by keeping the vehicle on the road. They maintained that passive suspension components are still very competitive, because they are simple, reliable and inexpensive and do not need a power supply, but the performance from the viewpoint of ride comfort is much worse when compared with the semi-active and active systems. Jian-Da et.al [13] proposed a semi-active vehicle suspension system using an adjustable shock absorber for a quarter-car model vibration control. Their results indicated that both PID Controller and the Fuzzy Controller effectively suppress the vibration of the quarter-car model. Most active suspensions require significant external power to function and that there is a considerable penalty in complexity, reliability, cost and weight. With a view to reducing complexity and cost while improving

ride comfort, handling and performance, the concept of piezoelectric exciter (piezoexciter) has emerge. In this kind of system, the conventional suspension spring and the shock absorber are retained, while the piezoexciter is fixed parallel to the spring and absorber.

This paper proposes an active vibration control scheme for controlling transverse vibration of rotor shaft due to mass unbalance and presents both theoretical and experimental studies. The use of piezoelectric actuators in active vibration control has been considered in the past by [14] and [15]. Yabuno et.al [16] used a piezoelectric actuator to stabilize the parametric resonance induced in a cantilever beam and to control bifurcation resulting in the shift of the bifurcation set and the expansion of the stable region. No attempt of vibration control of a quarter-car system by the use of a vertically placed piezoelectric exciter (that introduces parametric excitation force) has, however been reported to the authors' knowledge. Struble [17], Dugundji et.a[18], Chester[19] and Cartmell [20] have studied the effects of combined parametric and forced vibrations in dynamic systems. Mustafa & Ertas [21] theoretically and experimentally examined the effect of a pendulum (attached to the tip of a parametrically excited cantilever beam) whose natural frequency is tuned to be commensurable with a frequency of the beam in order to generate autoparametric resonance. For chosen external and internal resonance combinations, where the excitation frequency is twice the natural frequency of the first beam mode, and the linearised pendulum frequency is one-half that of the first beam mode, the results showed that, in some parametric excitation frequency ranges, the pendulum acts as vibration-absorbing device in the same manner as the pendulum attached to the main system under external excitation. The above ideas have led to the design of the piezoelectric exciter and the deliberate introduction of parametric excitations into a flexible rotor-bearing system axially to moderate the response of the pre-existing mass-unbalance vibration inherent to the rotor by [22] and [23]. The success of the above has led to the application of the piezoelectric exciter to the quarter-car to investigate the interactions between forced vibrations, which emanates from uneven road profile and parametric excitations, which results from the periodic stiffness variations caused by periodic vertical excitations from the actuator. The model of [2] is used with and without parametric force term in this paper. The method of Multiple Scales is used to solve the model equations to obtain the general solutions. Then *Mathematica*^{TM} Code is used evaluate the obtained MMS solutions with and without the excitation force term. Bifurcation analysis is also performed using *Mathematica*^{TM} and Dynamics 2 by Nusse and Yorke.

2 Mathematical Model of the Quarter-Car

The equation of motion of a modified single degree of freedom quarter-car model (Figure 1) of [2] is used and presented as

$$m\ddot{x} + k_1\left(x - x_0\right) + F_h = 0 \tag{1}$$

where, F_h is an additional nonlinear hysteretic suspension damping and stiffness force dependent on relative displacement and velocity, x_0 is the road excitation, x is the body's vertical displacement and m is the body mass.

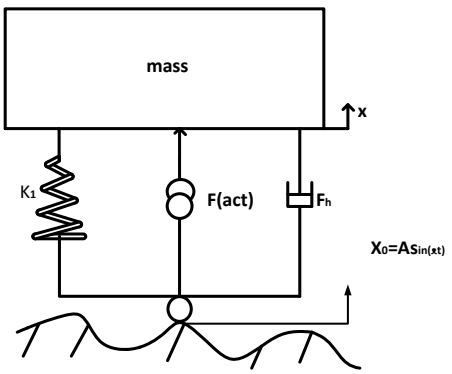

Figure 1. Modified 1DOF quarter-car model subjected to kinematic excitation with parametric exciter and nonlinear damping and stiffness.

Assuming $y = x - x_0$, $x_0 = A\sin\left(\Omega t\right)$ and $F_h = k_2\left(x - x_0\right)^3 + c_1\left(\dot{x} - \dot{x}_0\right) + c_2\left(\dot{x} - \dot{x}_0\right)^3$ Litak et. al. (2008), where, Ω is the excitation frequency and is equal to $\Omega = {2\pi v_0}/{\lambda}$, v_0 is the velocity of the car, A and λ are the amplitude and wavelength of the harmonic road profile, equation (1) can be rewritten as

$$\ddot{y} + \omega^2 y + B_1 y^3 + B_2 \dot{y} + B_3 \dot{y}^3 = A\Omega^2 \sin\left(\Omega t\right) \tag{2}$$

where, $\omega^2 = \frac{k_1}{m}$, $B_1 = \frac{k_2}{m}$, $B_2 = \frac{c_1}{m}$ and $B_3 = \frac{c_2}{m}$. The system's parameters are taken from [23] and are as follows: $m = 240\ kg$, $k_1 = 160000$ N/m , $k_2 = -300000$ N/m^3 , $C_1 = -250$ Ns/m , $C_2 = 25$ Ns^3/m^3 .

Adding the parametric term to equation (2), we get,

$$\ddot{y} + \omega^2 y + B_1 y^3 + B_2 \dot{y} + B_3 \dot{y}^3 - F_a \cos\left(\Omega_2 t\right) y = A\Omega^2 \sin\left(\Omega t\right) \tag{3}$$

where, $F_a \cos\left(\Omega_2 t\right) y$ is the parametric force term and F_a is the actuator force, where, $F_a = \frac{F_{act}}{m}$ and $\Omega_2 = 2\Omega$. Because of its simplicity, this model allows for a thorough examination of the parameters of the quarter-car vibration system, as well as the transition to a chaotic regime and the effect of the parametric excitation force. Although this simple model cannot simulate the detailed motion of a real vehicle, it can sufficiently approximate the dynamics to allow the results of analytic procedures performed on the simple nonlinear model to provide insight into the dynamics of the real vehicle.

3 Design and Selection of Piezoexciter Component

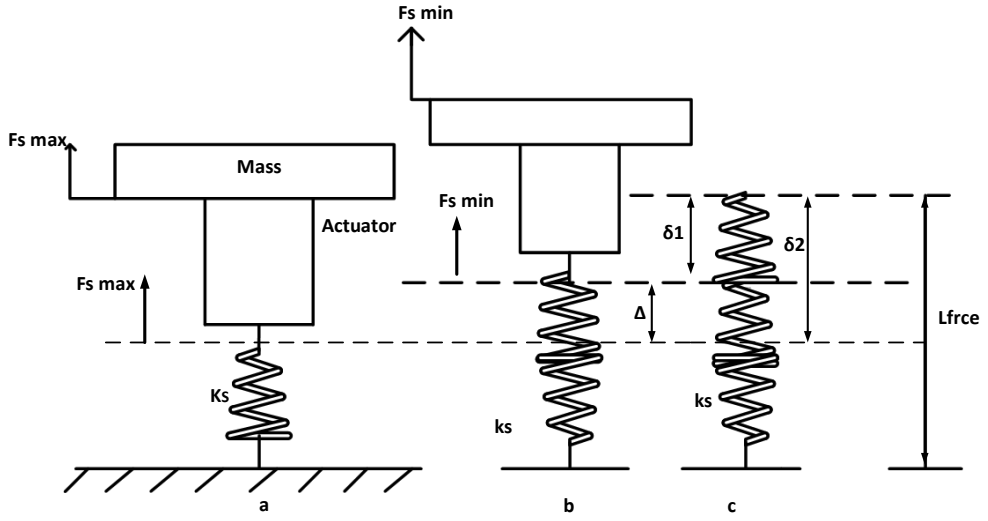

Figure 2. (a) Mass-Actuator assembly when the system is not excited. (b) Mass-Actuator assembly when the system is excited at maximum amplitude. (c) Free length of spring.

The actuator only displaces by micrometers so there will be a potential gap between the actuator and the base of the mass when the system is excited. The actuator will therefore have to follow the base of the mass as it gets displaced, but because the other end of the actuator has to react against something, a spring is needed to provide sufficient reaction, and to take up the space left as the mass moves upwards. The maximum spring force available is given in equation (4)

$$F_{s\max} = k_s \delta_2 \tag{4}$$

where, F_{smax} is the maximum spring force, k_s is the spring constant and δ_2 is the maximum spring compression. Figure 2(b) shows the mass having displace upwards as a consequence of the road

excitation. The spring has extended to fill the gap, Δ, and the remaining spring compression is δ_1. This is a pre-compression and is set up via equation (5) such that it satisfies the need for the minimum spring force (F_{smin}) offered by the spring to equal at least the maximum force which the actuator is capable of $F_{a(max),}$ meaning

$$F_{s\min} = F_{a(\max)} = k_s\delta_1 \tag{5}$$

where, δ_1 is the 'preload' pre-compression. As the minimum spring force available must be enough to resist the maximum force generated by the actuator, the actuator then can transmit its force to the mass, even when the mass has travelled by its maximum displacement upwards. The free length of the spring is as shown in Figure 2(c). It can easily be seen that the relationship between the pre-compression δ_1, the maximum compression δ_2, and the maximum displacement, Δ, is given by the equation (6)

$$\delta_1 = \delta_2 - \Delta \tag{6}$$

This means that the maximum spring force can be written as in equation (7)

$$F_{s\max} = k_s\left(\delta_1 + \Delta\right) \tag{7}$$

A spring was chosen based on the maximum required spring force and hence stiffness was obtained.

3.1 Maximum Spring Force

Equation (3) was used to find the parametric excitation force that is actually needed for the mass-spring quarter-car system, in order to get parametric resonances and the displacement due to the movement of the mass. The NDSolve integrator within *Mathematica*^{TM} code was employed to solve the differential equation. All other parameters were fixed and the parametric excitation force term value was varied until a parametric excitation plot was obtained as shown in Figure 3 and the value at which the response is predicted was taken as a threshold value for the parametric excitation force.

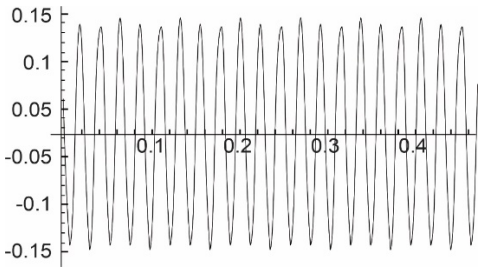

Figure 3. Parametric plot

From the above analysis, the maximum actuator force $F_{a\,(max)}$ is found to be $10,000$ N. Calculation of the maximum spring force is done using data from a realistic quarter-car model under construction at the Cape Coast Technical University and it is calculated using equations (4) to (7) and found to be $10,011.8$ N.

4 Approximate Analytical Solution to the Equations of Motion.

The Method of Multiple Scales (MMS) is used in solving equations (2) and (3). We nondimensionalise the time scale t and order the equations by introducing the small parameter ε. Let nondimensional time τ be $\tau = \omega t$, where, $\omega = \sqrt{\frac{k}{m}}$ and it is the natural frequency. ω is normalized to unity, therefore $\tau \equiv 1$ and letting $y = \varepsilon y$ and substituting across the equations (2) and (3) and solving give us the approximate solutions for the with and without the parametric excitation force terms. Equations (8) and (9) are the full time-domain solutions in the original parameters of equations (2) and (3) with and without parametric force term respectively. p, q, r and s are steady-state amplitudes.

$$y=\left\{\begin{array}{l}
2p\cos\left(\frac{\Omega t}{2\omega}\right)-2q\sin\left(\frac{\Omega t}{2\omega}\right)+\frac{B_1}{4\omega^2}p^3\cos\left(\frac{3\Omega t}{2\omega}\right)-\frac{3B_1}{4\omega^2}p^2q\sin\left(\frac{3\Omega t}{2\omega}\right)\\
-\frac{3B_1}{4\omega^2}pq^2\cos\left(\frac{3\Omega t}{2\omega}\right)+\frac{B_1}{4\omega^2}q^3\sin\left(\frac{3\Omega t}{2\omega}\right)+\frac{3B_1^2}{16\omega^4}p^5\cos\left(\frac{3\Omega t}{2\omega}\right)-\frac{9B_1^2}{16\omega^4}p^4q\sin\left(\frac{3\Omega t}{2\omega}\right)\\
-\frac{3B_1^2}{8\omega^4}p^3q^2\cos\left(\frac{3\Omega t}{2\omega}\right)-\frac{3B_1^2}{8\omega^4}p^2q^3\sin\left(\frac{3\Omega t}{2\omega}\right)-\frac{9B_1^2}{16\omega^4}pq^4\cos\left(\frac{3\Omega t}{2\omega}\right)+\frac{3B_1^2}{16\omega^4}q^5\sin\left(\frac{3\Omega t}{2\omega}\right)\\
-\frac{3B_1B_2}{32\omega^3}p^3\sin\left(\frac{3\Omega t}{2\omega}\right)-\frac{9B_1B_2}{32\omega^3}p^2q\cos\left(\frac{3\Omega t}{2\omega}\right)+\frac{9B_1B_2}{32\omega^3}pq^2\sin\left(\frac{3\Omega t}{2\omega}\right)+\frac{3B_1B_2}{32\omega^3}q^3\cos\left(\frac{3\Omega t}{2\omega}\right)\\
-\frac{3B_3\omega}{4}p^3\sin\left(\frac{3\Omega t}{2\omega}\right)-\frac{9B_3\omega}{4}p^2q\cos\left(\frac{3\Omega t}{2\omega}\right)+\frac{9B_3\omega}{4}pq^2\sin\left(\frac{3\Omega t}{2\omega}\right)+\frac{3B_3\omega}{4}q^3\cos\left(\frac{3\Omega t}{2\omega}\right)\\
+\frac{B_1^2}{32\omega^4}p^5\cos\left(\frac{5\Omega t}{2\omega}\right)-\frac{5B_1^2}{32\omega^4}p^4q\sin\left(\frac{5\Omega t}{2\omega}\right)-\frac{5B_1^2}{16\omega^4}p^3q^2\cos\left(\frac{5\Omega t}{2\omega}\right)+\frac{5B_1^2}{16\omega^4}p^2q^3\sin\left(\frac{5\Omega t}{2\omega}\right)\\
+\frac{5B_1^2}{32\omega^4}pq^4\cos\left(\frac{5\Omega t}{2\omega}\right)-\frac{B_1^2}{32\omega^4}q^5\sin\left(\frac{5\Omega t}{2\omega}\right)
\end{array}\right\} \quad (8)$$

$$y=\left\{\begin{array}{l}
2p\cos\left(\frac{\Omega t}{2\omega}\right)-2q\sin\left(\frac{\Omega t}{2\omega}\right)+\frac{B_1}{4\omega^2}p^3\cos\left(\frac{3\Omega t}{2\omega}\right)-\frac{3B_1}{4\omega^2}p^2q\sin\left(\frac{3\Omega t}{2\omega}\right)\\
-\frac{3B_1}{4\omega^2}pq^2\cos\left(\frac{3\Omega t}{2\omega}\right)+\frac{B_1}{4\omega^2}q^3\sin\left(\frac{3\Omega t}{2\omega}\right)+\frac{3B_1^2}{16\omega^4}p^5\cos\left(\frac{3\Omega t}{2\omega}\right)-\frac{9B_1^2}{16\omega^4}p^4q\sin\left(\frac{3\Omega t}{2\omega}\right)\\
-\frac{3B_1^2}{8\omega^4}p^3q^2\cos\left(\frac{3\Omega t}{2\omega}\right)-\frac{3B_1^2}{8\omega^4}p^2q^3\sin\left(\frac{3\Omega t}{2\omega}\right)-\frac{9B_1^2}{16\omega^4}pq^4\cos\left(\frac{3\Omega t}{2\omega}\right)+\frac{3B_1^2}{16\omega^4}q^5\sin\left(\frac{3\Omega t}{2\omega}\right)\\
-\frac{3B_1B_2}{32\omega^3}p^3\sin\left(\frac{3\Omega t}{2\omega}\right)-\frac{9B_1B_2}{32\omega^3}p^2q\cos\left(\frac{3\Omega t}{2\omega}\right)+\frac{9B_1B_2}{32\omega^3}pq^2\sin\left(\frac{3\Omega t}{2\omega}\right)+\frac{3B_1B_2}{32\omega^3}q^3\cos\left(\frac{3\Omega t}{2\omega}\right)\\
-\frac{3B_3\omega}{4}p^3\sin\left(\frac{3\Omega t}{2\omega}\right)-\frac{9B_3\omega}{4}p^2q\cos\left(\frac{3\Omega t}{2\omega}\right)+\frac{9B_3\omega}{4}pq^2\sin\left(\frac{3\Omega t}{2\omega}\right)+\frac{3B_3\omega}{4}q^3\cos\left(\frac{3\Omega t}{2\omega}\right)\\
+\frac{B_1^2}{32\omega^4}p^5\cos\left(\frac{5\Omega t}{2\omega}\right)-\frac{5B_1^2}{32\omega^4}p^4q\sin\left(\frac{5\Omega t}{2\omega}\right)-\frac{5B_1^2}{16\omega^4}p^3q^2\cos\left(\frac{5\Omega t}{2\omega}\right)+\frac{5B_1^2}{16\omega^4}p^2q^3\sin\left(\frac{5\Omega t}{2\omega}\right)\\
+\frac{5B_1^2}{32\omega^4}pq^4\cos\left(\frac{5\Omega t}{2\omega}\right)-\frac{B_1^2}{32\omega^4}q^5\sin\left(\frac{5\Omega t}{2\omega}\right)+\frac{3B_1F_aJ}{\Omega_2^2\omega^2+\Omega_2\omega^3}p^3\cos\left(\frac{5\Omega_2 t}{4\omega}\right)\\
-\frac{3B_1F_aJ}{\Omega_2^2\omega^2+\Omega_2\omega^3}p^2q\sin\left(\frac{5\Omega_2 t}{4\omega}\right)+\frac{3B_1F_aJ}{\Omega_2^2\omega^2+\Omega_2\omega^3}pq^2\cos\left(\frac{5\Omega_2 t}{4\omega}\right)-\frac{3B_1F_aJ}{\Omega_2^2\omega^2+\Omega_2\omega^3}q^3\sin\left(\frac{5\Omega_2 t}{4\omega}\right)\\
-\frac{B_2\Omega_2F_aJ}{\Omega_2^2\omega^2+2\Omega_2\omega^3}q\cos\left(\frac{5\Omega_2 t}{4\omega}\right)-\frac{B_2\Omega_2F_aJ}{\Omega_2^2\omega^2+2\Omega_2\omega^3}p\sin\left(\frac{5\Omega_2 t}{4\omega}\right)-\frac{B_2F_aJ}{\Omega_2^2\omega^2+2\Omega_2\omega^2}q\cos\left(\frac{5\Omega_2 t}{4\omega}\right)\\
-\frac{B_2F_aJ}{\Omega_2^2\omega^2+2\Omega_2\omega^2}p\sin\left(\frac{5\Omega_2 t}{4\omega}\right)-\frac{F_a^2N}{2\Omega_2^2\omega^2+4\Omega_2\omega^3}p\cos\left(\frac{9\Omega_2 t}{4\omega}\right)+\frac{F_a^2N}{2\Omega_2^2\omega^2+4\Omega_2\omega^3}q\sin\left(\frac{9\Omega_2 t}{4\omega}\right)
\end{array}\right\} \quad (9)$$

where, $J=\left[\frac{1}{-\frac{\Omega_2}{\omega^2}-\frac{2\Omega_2}{\omega}}\right]$ and $N=\left[\frac{1}{-\frac{4\Omega_2^2}{\omega^2}-\frac{4\Omega_2}{\omega}-1}\right]$.

5 Investigation of System's Dynamics

The models of the quarter-car system as equations (1) and (2) are used after some modifications for analysing the behaviour of the dynamical system using the *Dynamics 2* software and *Mathematica*^{TM} code. We therefore write the Model equations in the following form:

$$\ddot{y} + \bar{C}_1\dot{y} + \bar{C}_2\dot{y}^3 + \bar{C}_3 y + \bar{C}_4 y^3 = \rho\sin\left(\Omega t\right) \tag{10}$$

$$\ddot{y} + \bar{C}_1\dot{y} + \bar{C}_2\dot{y}^3 + \bar{C}_3 y + \bar{C}_4 y^3 - \bar{C}_5 y\cos\left(\Omega_2 t\right) = \rho\sin\left(\Omega t\right) \tag{11}$$

where, $\bar{C}_1 = \frac{c_1}{m}$; $\bar{C}_2 = \frac{c_2}{m}$; $\bar{C}_3 = \frac{k_1}{m}$; $\bar{C}_4 = \frac{k_2}{m}$; $\bar{C}_5 = F_a$; $\rho = \frac{A\Omega^2}{m}$; ρ is the excitation amplitude, Ω is the excitation frequency, Ω_2 is the parametric excitation frequency.

5.1 Nondimensionalization

The time t is nondimensionalised by using the rotor system natural frequency ω. Nondimensionalisation of the timescale in equations (10) and (11) is introduced by stating $\tau = \sqrt{\omega}t$, where, ω is the natural frequency of the first mode of the flexible rotor system. Therefore,

$$\ddot{y} = \frac{d^2y}{dt^2} = \frac{d^2y}{d\left(\frac{\tau}{\sqrt{\omega}}\right)^2} = \frac{\omega d^2y}{d\tau^2} \therefore \ddot{y}\left(t\right) = \omega y''\left(\tau\right) \tag{12}$$

$$\dot{y} = \frac{dy}{dt} = \frac{dy}{d\left(\frac{\tau}{\sqrt{\omega}}\right)} = \frac{\sqrt{\omega}dy}{d\tau} \therefore \dot{y}\left(t\right) = \sqrt{\omega}y'\left(\tau\right) \tag{13}$$

In terms of the dimensionless timescale, τ, equations (10) and (11) become

$$\omega y'' + \sqrt{\omega}\bar{C}_1 y' + \left(\sqrt{\omega}\right)^3 \bar{C}_2 y' + \bar{C}_3 y + \bar{C}_4 y^3 = \rho\sin\left(\frac{\Omega}{\sqrt{\omega}}\right)\tau \tag{14}$$

$$\omega y'' + \sqrt{\omega}\bar{C}_1 y' + \left(\sqrt{\omega}\right)^3 \bar{C}_2 y' + \bar{C}_3 y + \bar{C}_4 y^3 - \bar{C}_5 y\cos\left(\frac{\Omega_2}{\sqrt{\omega}}\right)\tau = \rho\sin\left(\frac{\Omega}{\sqrt{\omega}}\right)\tau \tag{15}$$

where the prime (') denotes differentiation with respect to dimensionless time τ. Dividing equations (14) and (15) by ω, gives

$$y'' + C_1 y' + C_2 y' + C_3 y + C_4 y^3 = \frac{\rho}{\omega}\sin\left(phit\right) \tag{16}$$

$$y'' + C_1 y' + C_2 y' + C_3 y + C_4 y^3 - C_5 y\cos\left(2phit\right) = \frac{\rho}{\omega}\sin\left(phit\right) \tag{17}$$

where, $C_1 = \frac{\bar{C}_1}{\sqrt{\omega}}$; $C_2 = \sqrt{\omega}\bar{C}_2$; $C_3 = \frac{\bar{C}_3}{\omega}$; $C_4 = \frac{\bar{C}_4}{\omega}$; $C_5 = \frac{\bar{C}_5}{\omega}$; $phi = \phi = \Omega$

The second order ordinary differential equations are then split into first order ordinary differential equations making them more compact. $y' = v$

$$v' = \frac{\rho}{\omega}\sin(\phi t) - C_1 v - C_2 v - C_3 y - C_4 y^3 \tag{18}$$

$$v' = \frac{\rho}{\omega}\sin(\phi t) - C_1 v - C_2 v - C_3 y - C_4 y^3 + C_5 y\cos(\phi_2 t) \tag{19}$$

These first order equations are then used to calculate time response, phase plane trajectories and predictions of Bifurcations.

The parameter values for the program codes are presented in Table 1 for the models of coupled equations with and without the parametric force term, corresponding to all the data described in section 2.

Table 1. Data used for numerical simulations

	Dimensional	**Nondimensional**
Stiffness (Linear)	$\overline{C}_3 = 585.6\ [s^{-2}]$	$C_3 = 22.7$
Damping Coefficient	$\overline{C}_1 = -1.04\ [s^{-1}]$	$C_1 = -0.205$
Nonlinear Damping Coefficient	$\overline{C}_2 = 0.104\ [s^{-3}]$	$C_2 = 0.528$
Stiffness (Cubic)	$\overline{C}_4 = -1250\ [m^{-2}s^{-2}]$	$C_4 = -48.45$
Actuator Force	$\overline{C}_5 = 41.7\ [ms^{-2}]$	$C_5 = 1.62$
Excitation Amplitude	$\overline{\rho} = 0.277\ [ms^{-2}]$	$\frac{\rho}{\omega} = 0.01$
Excitation Frequency	$\Omega = \phi = 25.8\ [rads^{-1}]$	
Parametric Frequency	$\Omega_2 = \phi_2 = 51.6\ [rads^{-1}]$	

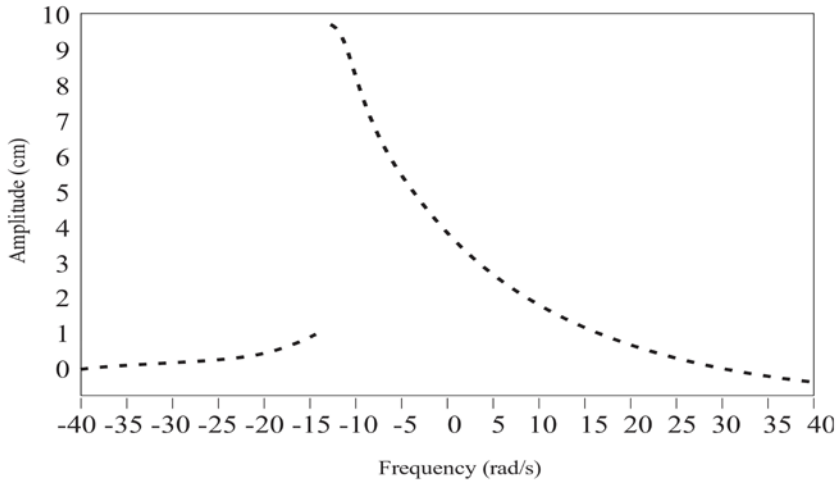

Figure 4. Amplitude of the response as a function of the frequency-without parametric force term.

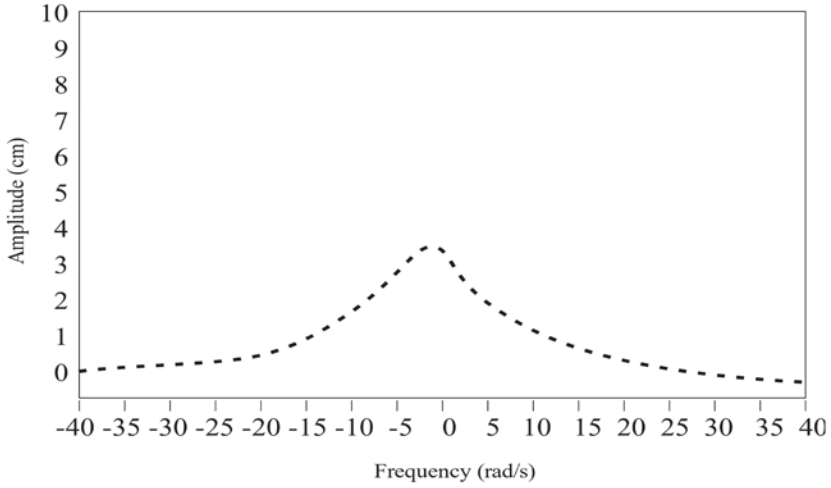

Figure 5. Amplitude of the response as a function of the frequency-with parametric force term.

6 Results and Analysis

In Figures 4 and 5, each dot on the curves corresponds to a singular point. Figure 4 shows a plot of amplitude y versus forcing frequency Ω when the amplitude of excitation A=0.3 m (i.e. where the strongest nonlinear response is observed). A Peak amplitude vibration of 9.8 cm is observed. The well-known jump phenomenon indicating instability is observed. In Figure 5, including parametric force term in the model equation, and at the amplitude of excitation A=0.3 m, the amplitude of vibration reduced to 3.5 cm. It is also observed that the jump is eliminated and the peak amplitude of vibration of the motion is reduced by approximately 64.3%.

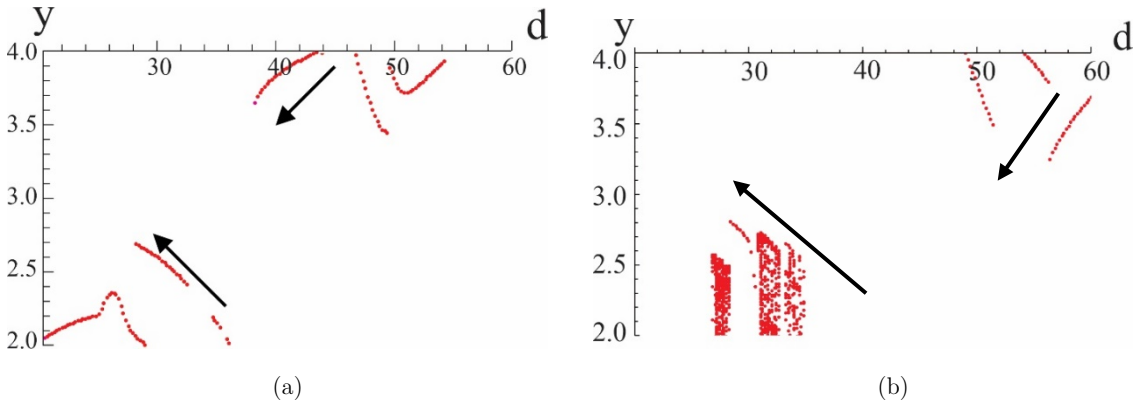

Figure 6. Bifurcation diagrams of amplitude as a function of the nondimensionalised excitation acceleration for the model without parametric force term at (a) the amplitude of a road profile at A=0.1m; (b) the amplitude at A=0.3m.

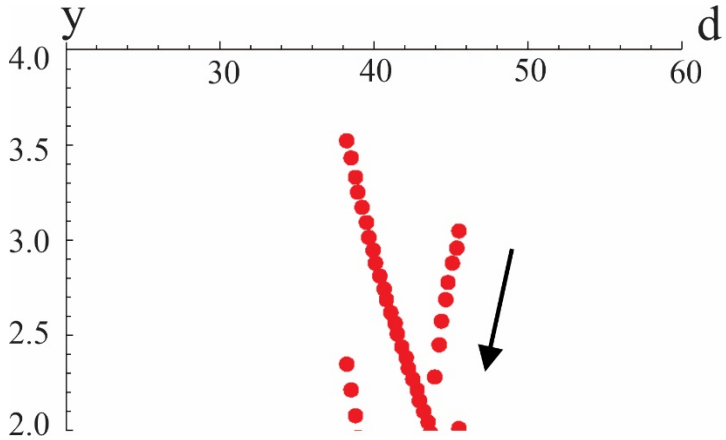

Figure 7. Bifurcation diagram of amplitude as a function of the nondimensionalised excitation acceleration for the model with parametric force term at amplitude of a road profile A=0.3m.

Figures 6 and 7 show bifurcation diagrams of amplitude as controlled by the nondimensionalised excitation acceleration, when the excitation is set equal to the resonance frequency. In this work for the physical system to become more intrinsically nonlinear, the excitation amplitude value have to be increased to various multiples of the actual value. This effect causes the system to show possible bifurcations to chaos. The periodic response for the case based on the smallest amplitude A=0.1 m in Figure 6 (a) (i.e. the most weakly nonlinear response), bifurcates to chaos as the amplitude of the road profile increases to A=0.3 m in Figure 6 (b), at dominant Lyapunov exponents of $\lambda_1 = -0.1405$ and $\lambda_1 = 0.0124$, respectively. The arrows indicate excitation acceleration reduces in the simulations.

Negative Lyapunov exponents show stable motion, while the positive Lyapunov exponents show clear indications of chaos.

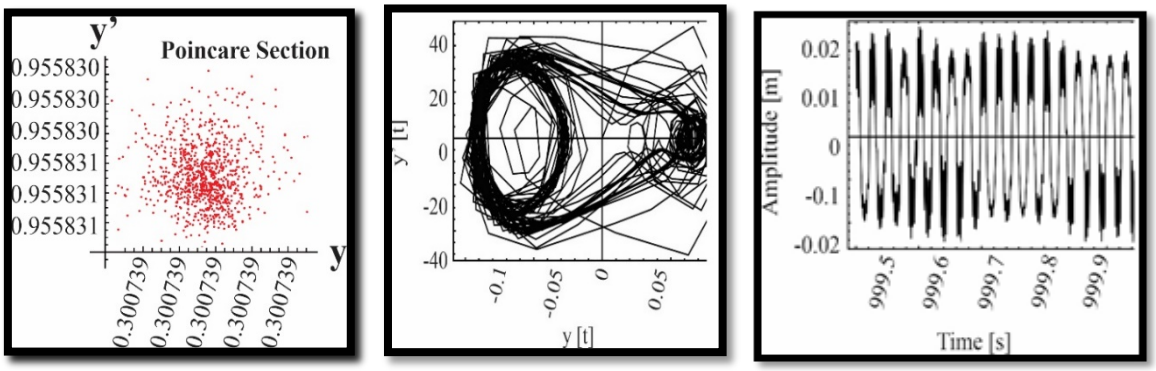

(a) (b) (c)

Figure 8. Poincare Map (a), Phase Plane (b) and Time Plot (c) the nondimensionalised excitation acceleration for the model without parametric force term at amplitude of a road profile A=0.3m

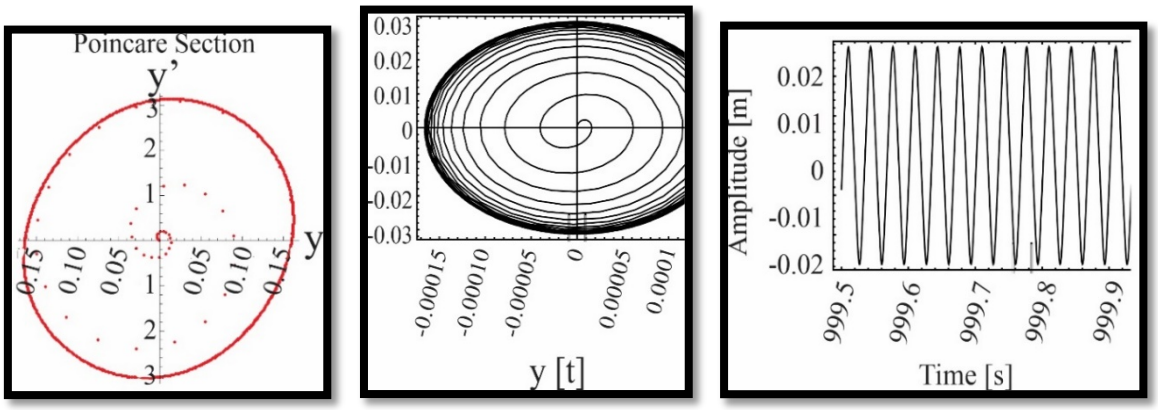

(a) (b) (c)

Figure 9. Poincare Map (a), Phase Plane (b) and Time Plot (c) the nondimensionalised excitation acceleration for the model with parametric force term at amplitude of a road profile A=0.3m.

Figure 7 shows the bifurcation as controlled by nondimensionalised excitation acceleration, and using the resonance frequency ($\boldsymbol{\Omega}$) value, when a parametric force term is included at a parametric frequency of twice the resonance frequency value. By increasing the amplitude value to A=0.3 m, the periodic responses remain periodic. The bifurcation diagram did not change qualitatively, while the negative Lyapunov exponent of $\lambda_1 = -0.0492$ show stable periodic motion. This means upon including the parametric force term in the system the chaotic motion present in the quarter-car system, and observed in Figure 6 (b), becomes stable. This indicates that the chaotic motion, which is bounded by the bifurcation set, is automatically shifted resulting in stable periodic motion.

The analysis of Figures 6 and 7 are extended to Phase planes, Poincare maps and Time plots (i.e. Figures 8 and 9). The Phase planes and Time plots are plotted at assumed steady-state conditions, taken to be during the interval $t = 995 - 1000$ second. However, the Poincare maps are plotted from the transient time (i.e. $t = 0 - 1000$ seconds). The plots are found in a number of regular and irregular points. At nondimensionalised excitation acceleration for the model without parametric force term at amplitude of A=0.3 m, the bifurcation diagram in Figure 6 (b) shows a chaotic motion with positive Lyapunov exponent. Its corresponding Poincare map (Figure 8 (a)) shows irregular scattered points and is that of chaotic motion. The Phase Plane (Figure 8 (b)) underpin the above. The plots have overlaid,

complicated and repeated orbit cross-overs. In Figure 8 (c), the Time plot is non-periodic, the oscillations do not repeat and is another qualitative visual indicator of chaotic motion. At nondimensionalised excitation acceleration for the model with parametric force term at amplitude of A=0.3 m, the bifurcation diagram in Figure 7 shows stable periodic motions with negative Lyapunov exponents. Its corresponding Poincare map, Phase Plane and Time plot in Figure 9 (a), (b) and (c) respectively display stable periodic motions.

7 Conclusion

Chaotic vibrations of a quarter-car model excited by the road surface is studied in this paper. The equation of motion and parameters used were taken from [24] was modified to include a parametric excitation force term to enable the manipulation of the system's behavior. The simple model approximates the dynamics sufficiently to provide insight into the dynamics of the real vehicle. The results from the multiple scales analysis show evidence of a phenomenon whereby the responses of the amplitudes show softening characteristics, jump phenomenon and stable and unstable solutions when the equations of motion contain no parametric force term. Including parametric force term, the solution shows decrease in amplitude value by 64.3%, elimination of the jump phenomenon and stable solutions. The numerical results show similar trends with the multiple scales results. In this studies chaos is evident as the system becomes more nonlinear due to increase in excitation amplitude values and that with the introduction of parametric force term the system's motion becomes periodic. Comparing the piezoelectric exciter (piezoexciter) concept to the other methods mentioned in the introduction especially the magnetorheological dampers, which seem to be very popular, the piezoexciter concept comes with reducing complexity and cost while improving ride comfort, handling and performance.

References

1. G. Verros, S. Natsiavias, and G. Stepan, "Control and dynamics of quarter-car model with dual-rate damping", *Journal of Vibration Control*, Vol.6, pp.1045-1063, 2000.
2. S. Li, S. Yang and W. Guo, "Investigation on chaotic motion in hysteretic non-linear suspension system with multi-frequency excitations," *Mech. Res. Commun*, Vol.31, pp.229-236, 2004.
3. D. L. Guo, H. Y. Hu and J. Q. Yi, "Neural network control for a semi-active vehicle suspension with a magnetorheological damper," *Journal of Vibration Control*, Vol. 10, pp. 461-471, 2004.
4. C. Lauwerys, J. Swevers and P. Sas, "Robust linear control of an active suspension on a quarter-car test-rig," *Control Engineering Practice*, Vol.13, pp. 577-586, 2005.
5. K. Szabelski, "The vibrations of self-excited system with parametric excitation and non-symmetric elasticity characteristics," *J Theor. Appl. Mech*, Vol.29; pp. 57-81,1991.
6. M. Mitschke, "Dynamik der Kraftfahrzeuge", Berlin: Springer, 1990.
7. S. B. Choi and S. K. Lee, "A hysteresis model for the field-dependent damping force of a magnetorheological damper," *Journal of Sound and Vibration*, Vol. 245; pp.375-383, 2001.
8. C.Y. Lai C.Y and W.H. Liao, "Vibration control of a suspension system via a magnetorhellogical fluid damper," *Journal of Vibration Control*, Vol. 8, pp. 527-547, 2002.
9. D. C. Karnopp, M. J. Crosby and R. A. Harwood, "Vibration control using semi-active force Generators," *Trans ASME, J Eng. Ind*. pp. 619-626, 1974.
10. P. Soravia, "H ∞ control of nonlinear systems: differential games and viscosity solutions," *SIAM. J Control Optim*, Vol. 34, pp. 1071-1097, 1996.
11. V. S. Dixit and S. C. Borse, "Semi-active suspension system design for quarter-car model and its analysis with passive suspension model," *Int. J of Eng. Sci. & Res. Tech. (IJESRT)*, Vol. 6 (2), pp. 203-211, 2017.
12. V.K. Allamraju, "Modal analysis of quarter car model suspension system," *Int. J of Eng. Sci. & Res. Tech. (IJESRT)*, Vol. 5 (7), pp. 1216-1224, 2016.
13. W. Jian-Da, L. Chih-Jer and K. Kun-Yin, "A study of semi-active vibration control for vehicle suspension system using an adjustable shock absorber," *Journal of low Frequency Noise, Vibration and Active Control*, Vol. 27(3), pp. 219-235, 2008.

14. A. B. Palazzolo, S. Jogannathan, A. F. Kascak, G.T. Montague and L.J. Kiraly, "Hybrid active vibration control of rotor bearing systems using piezoelectric actuators," *Journal of vibration and Acoustics*; Vol.115, pp. 111-119, 1993.
15. T. S. Barre, A. B. Palazzolo and A.F. Kascak, "Active vibration control of rotating machinery using piezoelectric actuators incorporating flexible casing effects," *Trans.ASME, J. Eng. Gas Turbine Power, Vol.* 117 pp.176-187, 1993.
16. H. Yabuno, S. Saigusa, and N. Aoshima, "Stabilization of the parametric resonance of a cantilever beam by bifurcation control with a piezoelectric actuator," Nonlinear *Dynamics*, Vol. 26, pp. 143-161, 2001.
17. R. A. Struble, "On the subharmonic oscillations of a pendulum," *ASME Journal of Applied Mechanics*, Vol.30, pp. 301-303, 1963.
18. J. Dugundji and C. K. Chhatpar, "Dynamic stability of a pendulum under parametric excitation," *Rev. Sci. Tech., Ser. Mech. Appl.*, Vol.15 (4), pp. 741-763,1970.
19. W. Chester, "The forced oscillations of a simple pendulum," Journal *of Inst. Math. Applications*; Vol.15, pp. 289-306, 1975.
20. M. P. Cartmell, "Introduction to linear, parametric and nonlinear vibrations," *Chapman and Hall*, London, 1990.
21. G. Mustafa and A. Ertas, "Dynamics and bifurcations of a coupled column-pendulum oscillator," *Journal of Sound and Vibration*, Vol.182 (3), pp. 393-413, 1994.
22. L. Atepor, "Vibration analysis and intelligent control of flexible rotor systems using smart materials," *Ph.D. Thesis, University of Glasgow, U.K., 2008.*
23. L. Atepor, "Controlling Flexible Rotor Vibrations Using Parametric Excitation," *7th International Conference on Modern Practice in Stress and Vibration Analysis IOP Publishing. Journal of Physics,* Conference Series 181 (2009) 012021 doi:10.1088/1742-6596/181/1/012021.
24. G. Litak, M. Borowiec, M. I. Friswel and K. Szabelski, (2008). "Chaotic vibration of a quarter-car model excited by the road surface profile," *Communications in Nonlinear Science and Numerical Simulation,* Vol. 13, pp.1373-1383, 2008.

